Cell

Cernunnos, a Novel Nonhomologous End-Joining Factor, Is Mutated in Human Immunodeficiency with Microcephaly

Dietke Buck,[1] Laurent Malivert,[1] Régina de Chasseval,[1] Anne Barraud,[1] Marie-Claude Fondanèche,[1] Ozden Sanal,[2] Alessandro Plebani,[3] Jean-Louis Stéphan,[4] Markus Hufnagel,[5] Françoise le Deist,[1,6] Alain Fischer,[1,6] Anne Durandy,[1,6] Jean-Pierre de Villartay,[1,6,*] and Patrick Revy[1]

[1] INSERM, Hôpital Necker-Enfants Malades, U768 Unité Développement Normal et Pathologique du Système Immunitaire, Paris, F-75015 France; Université Paris Descartes, Faculté de Médecine René Descartes, Paris, F-75005 France

[2] Immunology Division, Hacettepe University, Ankara, Turkey

[3] Clinica Pediatrica and Istituto di Medicina Moleculare "Angelo Nocivelli," Università di Brescia, Italy

[4] Unité d'Hématologie et Oncologie Pédiatrique, CHU Saint Etienne, France

[5] Children's Hospital, Department of General Pediatrics, University Hospital Schleswig-Holstein, Campus Kiel, Germany

[6] AP/HP, Hôpital Necker-Enfants Malades, Unité d'Immunologie et d'Hématologie, Paris, F-75015 France

*Contact: devillar@necker.fr

DOI 10.1016/j.cell.2005.12.030

SUMMARY

DNA double-strand breaks (DSBs) occur at random upon genotoxic stresses and represent obligatory intermediates during physiological DNA rearrangement events such as the V(D)J recombination in the immune system. DSBs, which are among the most toxic DNA lesions, are preferentially repaired by the nonhomologous end-joining (NHEJ) pathway in higher eukaryotes. Failure to properly repair DSBs results in genetic instability, developmental delay, and various forms of immunodeficiency. Here we describe five patients with growth retardation, microcephaly, and immunodeficiency characterized by a profound T+B lymphocytopenia. An increased cellular sensitivity to ionizing radiation, a defective V(D)J recombination, and an impaired DNA-end ligation process both in vivo and in vitro are indicative of a general DNA repair defect in these patients. All five patients carry mutations in the *Cernunnos* gene, which was identified through cDNA functional complementation cloning. Cernunnos/XLF represents a novel DNA repair factor essential for the NHEJ pathway.

INTRODUCTION

DNA double-strand breaks (DSBs) are among the most toxic DNA lesions caused by cell-intrinsic sources such as replication errors or other DNA-damaging agents naturally present in cells, including reactive oxygen species. DSBs can also result from exposure to a variety of extrinsic factors, including ionizing radiation (IR). Lastly, DSBs represent obligatory intermediates of physiological DNA rearrangement processes taking place during the development and maturation of the adaptive immune system (V[D]J recombination and immunoglobulin [Ig] heavy chain class switch recombination [CSR]) (Sancar et al., 2004). The V(D)J recombination is a somatic DNA rearrangement of *V*ariable, *D*iversity, and *J*oining gene segments encoding the T and B cell antigen receptor loci. The lymphoid-specific recombination activating gene (*RAG*) 1 and 2 encoded endonuclease initiates the reaction by introducing a DSB at recombination-specific sequences (RSS) that flank all V, D, and J gene units (Bassing et al., 2002). The efficient repair of DNA DSBs introduced during these reactions is required to maintain genome integrity, thus preventing the development of cancer and other "DNA instability" disorders. DSBs are primarily repaired by the accurate homologous recombination (HR) in yeast and by the error-prone nonhomologous end-joining (NHEJ) pathway in higher eukaryotes (Sancar et al., 2004). To date, six mammalian factors have been identified as constituting the core NHEJ apparatus involved in V(D)J recombination. The Ku70/Ku80 heterodimer binds to DNA ends, present at RAG1/2-generated DSBs, and recruits the ATM-related kinase DNA-PKcs (Gottlieb and Jackson, 1993; Dynan and Yoo, 1998). DNA-PKcs then phosphorylates and activates the Artemis endonuclease, the enzyme required to resolve DNA hairpin structures created upon RAG1/2-specific DNA cleavage (Ma et al., 2002). The XRCC4/DNA-LigaseIV (Lig4) complex is responsible for the final ligation step (Grawunder et al., 1997).

The fundamental role of NHEJ factors in the immune system has been recognized through genetic deletion in mice and studies of specific human conditions (de Villartay et al., 2003). In all animal models, NHEJ defects result in the arrest of B and T lymphocyte maturation, accompanied by an embryonic lethality in the case of XRCC4 and Lig4 deficiencies (Dudley et al., 2005; Revy et al., 2005). In humans, null mutations in

Table 1. Clinical Features of Patients

Patients	Origin	Consanguinity	Microcephaly	Growth Retardation	Associated Clinical Features	Infections	Autoimmunity	Outcome
P1	French	no	yes	yes	chromosomal alterations, urogenital and bone malformations	bacterial and opportunistic	autoimmune anemia and thrombocytopenia	died at 18 years: septic shock
P2	Turkish	+, 1st degree	yes	yes	no	bacterial and opportunistic	no	died at 4 years: septic shock
P3*	Turkish	+, 1st degree	yes	yes	birdlike face, bone malformation	bacterial and opportunistic	autoimmune anemia and thrombocytopenia	alive: 14 years old
P4*	Turkish	+, 1st degree	yes	yes	birdlike face	bacterial and opportunistic	no	alive: 3 years old
P5	Italian	+, 3rd degree	yes	yes	birdlike face, chromosomal alterations, bone marrow aplasia	recurrent respiratory tract infections	no	alive: 9 years old

* P3 and P4 are siblings.

Artemis result in RS-SCID, characterized by a complete absence of peripheral T and B lymphocytes and an increased cellular sensitivity to IR (Moshous et al., 2001). Variable immunodeficiency, developmental delay, chromosome alterations, and microcephaly have also been attributed to hypomorphic mutations in the *Lig4* gene in humans (O'Driscoll et al., 2001; Buck et al., 2006). Finally, a radiosensitive SCID condition (patient 2BN) without mutation in any of the known NHEJ factors was identified, supporting the existence of additional uncharacterized DNA repair factors (Dai et al., 2003).

With the aim of identifying new factors involved in general DNA repair, we undertook a systematic survey of human conditions characterized by developmental anomalies, such as microcephaly, associated with various degrees of immune deficiency and/or the onset of lymphopoietic malignancy. In this article, we describe a new syndrome of human combined immunodeficiency (CID) associated with microcephaly and increased cellular sensitivity to IR. This condition is caused by a general DNA repair defect owing to mutations in a novel NHEJ factor encoding gene, *Cernunnos*.

RESULTS

A New Syndrome Associated with T and B Cell Combined Immunodeficiency, Growth Retardation, and Microcephaly

The main clinical features characterizing the patients included in this study were growth retardation, microcephaly, and immunodeficiency (for detailed case reports, see Experimental Procedures and Tables 1 and 2). Severe growth retardation and dystrophy were observed in four of the five patients, and microcephaly was present in all five patients at birth. Dysmorphic features and various malformations were observed in four of the patients (Table 1). Recurrent infections of bacterial, viral, and/or parasitic origin occurred in all patients and were lethal in two. Laboratory analysis indicated a mild to severe B (CD19+) and T (CD3+) lymphocytopenia in all patients, whereas the NK cell subset was not affected (Table 2). Circulating B cell counts declined with age from close to normal values to undetectable levels, and most patients displayed hypogammaglobulinemia affecting IgG and IgA, accompanied by fluctuating levels of IgM (Table 2). The T lymphocyte subsets were composed only of memory T cells (CD45RO positive) with impaired functions determined by low in vitro PHA mitogen-induced T cell proliferation.

In association with microcephaly, the absence of circulating naïve T cells and the progressive disappearance of B cells were indicative of a molecular defect affecting the maturation of the immune system as observed in Lig4 deficient or Nijmegen breakage syndrome (NBS) patients.

Increased Radiosensitivity of Patients' Fibroblasts

Lig4 and NBS conditions are two DNA repair deficiencies characterized by an increased cellular sensitivity to IR (Varon et al., 1998; O'Driscoll et al., 2001; Buck et al., 2006). Primary skin fibroblasts from four of the tested patients (P1-P4) exhibited an increased sensitivity to γ ray exposure as

Table 2. Immunological Characteristics of Patients

Patients	P1	P2	P3	P4	P5
Age at diagnosis (years)	14	2	13	2	7
Lymphocyte counts[a]	750 (*1400–3300*)	1220 (*2300–5400*)	1610 (*1400–3300*)	2570 (*2300–5400*)	1101 (*1900–3700*)
T lymphocytes[a]	630 (*1000–2200*)	730 (*1400–3700*)	870 (*1000–2200*)	591 (*1400–3700*)	693 (*1200–2600*)
T CD4+[a]	428 (*530–1300*)	150 (*650–1500*)	490 (*530–1300*)	334 (*650–1500*)	319 (*530–1300*)
CD45RO/T CD4 (%)	99 (*18–38*)	98 (*9–26*)	87 (*18–38*)	98 (*9–26*)	99 (*13–30*)
T CD8+[a]	248 (*330–920*)	559 (*370–1100*)	370 (*330–920*)	77 (*370–1100*)	330 (*330–920*)
CD45RO/T CD8 (%)	92 (*4–23*)	54 (*4–16*)	65 (*4–23*)	n.i.	83 (*4–21*)
B lymphocytes[a]	0 (*110–570*)	75 (*390–1400*)	0 (*110–570*)	154 (*390–1400*)	44 (*110–570*)
NK cells[a]	n.d.	281 (*92–918*)	402 (*42–726*)	1336 (*92–918*)	195 (*76–629*)
T cell proliferation PHA[b]	30 (*>40*)	5.8 (*>40*)	119 (*>40*)	84 (*>40*)	16 (*>40*)
Ig values before substitution					
IgG[c]	2.4 (*6.4–14.2*)	<0.33 (*5.2–10.8*)	<0.5 (*2.8–6.8*)*	2.37 (maternal; *2.7–5.3*)**	0.6 (*5.7–13.2*)
IgA[c]	<0.06 (*0.52–2.2*)	<0.06 (*0.36–1.65*)	<0.5 (*0.1–0.58*)*	<0.05 (*0.02–0.22*)**	0.06 (*0.65–2.4*)
IgM[c]	6.8 (*0.4–1.8*)	1.39 (*0.72–1.60*)	0.15 (*0.4–0.84*)*	0.27 (*0.36–0.56*)**	1.05 (*0.6–1.75*)

n.d.: not done.
n.i.: not interpretable.
Age-matched control values are from Shearer et al. (Shearer et al., 2003) and are shown in italics in parentheses. Tested at *5 or **3 months of age.
[a] in counts/μl; presence of maternal T cells was excluded by HLA typing of sorted T cells.
[b] Phytohemagglutinin (PHA)-induced proliferations are expressed as counts per minute × 10^{-3}.
[c] in mg/ml.

compared to control cells in a clonogenic assay (Figure 1A). Although the level of IR sensitivity was variable among the patients, it was equivalent or sometimes more pronounced than what was observed in other radiosensitive conditions, such as Ataxia telangiectasia (A-T), NBS, Lig4, or Artemis deficiencies (Figure 1A and data not shown).

IR-Induced Foci Formation Is Normal in Patients' Fibroblasts

The phosphorylation of the histone variant H2AX (then called γH2AX) occurs rapidly in response to a DNA-DSB (Rogakou et al., 1998) and is essential to keeping DNA ends in close proximity and to stabilizing the association of DNA-repair factors such as the MRE11-RAD50-NBS1 (MRN) complex and 53BP1 at the site of the damage (Bassing and Alt, 2004), forming ionizing radiation-induced foci (IRIF). γH2AX, MRE11, 53BP1, and RAD51 IRIFs were equally well formed in P1-P4 and control fibroblasts 2 hr after 10 Gy irradiation (Figures 1B and S1 and data not shown). This result suggests that the increased sensitivity to IR does not result from a defect in the initial DNA damage sensing. In contrast to normal control cells, γH2AX signal persisted in patients' cells 24 hr following DSB induction, as observed by both microscopy and fluorocytometry, signifying a major DNA repair defect in these cells (Figure 1B and data not shown).

Normal Cell-Cycle Checkpoints in Patients' Fibroblasts Following IR

IR induce cell-cycle checkpoints, which can be analyzed at three critical steps: the inhibition of entry into the S phase (G1/S checkpoint), the S phase progression, and the inhibition of entry into mitosis (G2/M checkpoint). The G1/S checkpoint following a 5 Gy IR was comparable in all patients' and controls' fibroblasts with a 75% mean inhibition of S phase entry (Figures 1C and 1D). This contrasted with the defect of this checkpoint in fibroblasts from A-T or NBS patients (Figures 1C and 1D). The S phase progression, analyzed through radioresistant DNA synthesis (RDS) assay, was also similarly inhibited in patients' and controls' fibroblasts following IR (Figure S2). Lastly, we examined the IR-induced G2/M checkpoint by analyzing the phosphorylation of the Histone 3 (H3) (Figure 1E). H3 phosphorylation (P-H3)

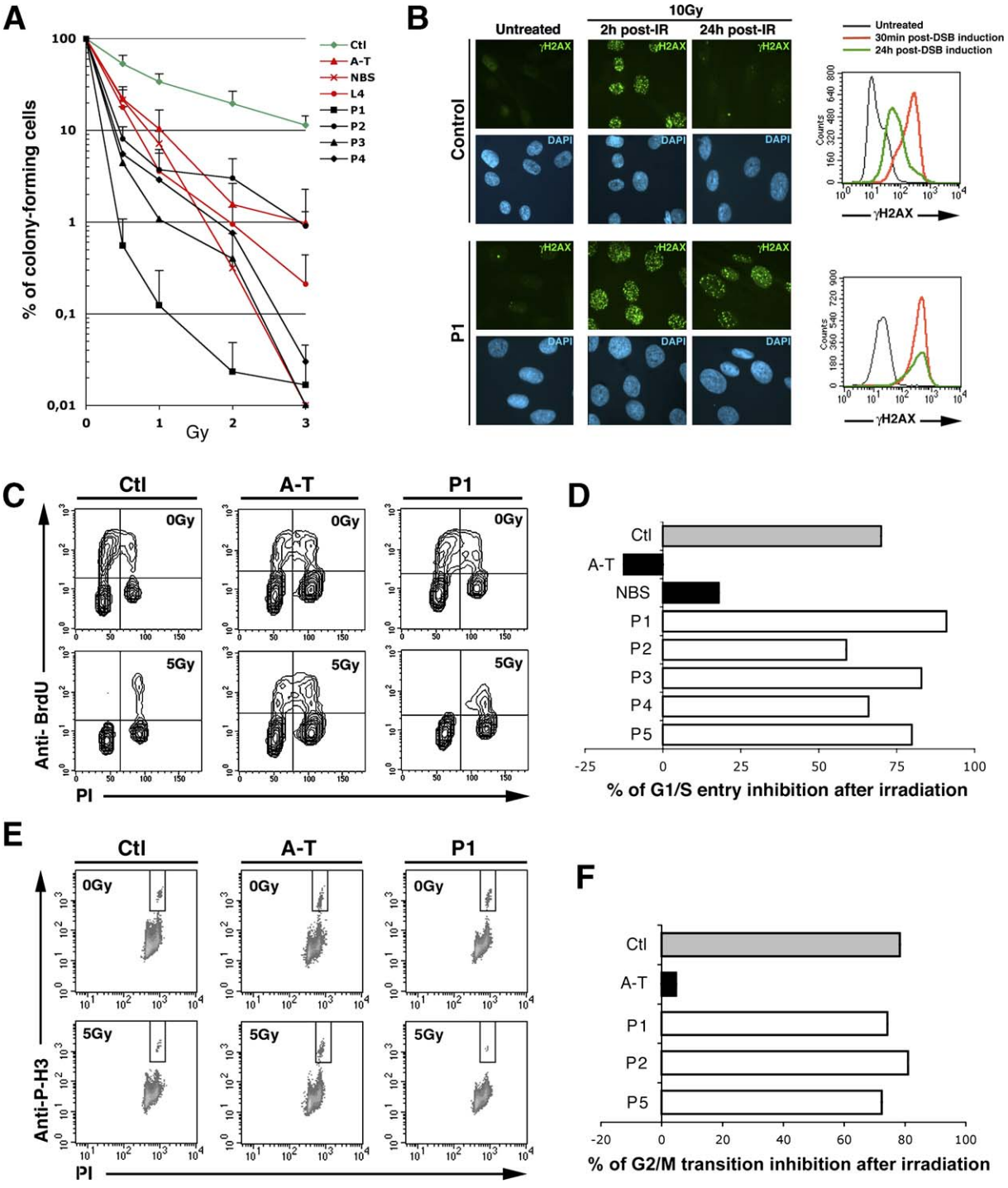

Figure 1. Cellular Response to DNA Damage

(A) Survival of primary fibroblasts after IR (up to 3 Gy). Results are expressed as the fraction of colony-forming cells in relation to unirradiated cells. Each point represents the mean value and standard deviation of three separate determinations. Control radiosensitive fibroblasts were from Lig4 (L4), A-T, and NBS patients.

(B) Left panel: Primary fibroblasts from the control and P1 were seeded onto glass slides and either left untreated or else irradiated with 10 Gy and fixed 2 or 24 hr postirradiation before staining with anti-γH2AX. Nuclei were stained with DAPI. Right panel: γH2AX detection by fluorocytometry was performed in untreated fibroblasts (black curve) and 30 min (red curve) or 24 hr (green curve) post-DSB induction. Persistence of γH2AX signal at 24 hr posttreatment in patients' cells in both experiments is indicative of a general DNA-repair defect.

correlates with chromosome condensation occurring immediately before mitosis (Wei et al., 1999). The 80% decrease in P-H3-positive cells in patients' and controls' fibroblasts following a 5 Gy IR (Figures 1E and 1F) indicated a normal G2/M checkpoint and contrasted with the impaired G2/M checkpoint in A-T cells. Altogether, these results demonstrated that the IR-induced biochemical events leading to the various cell-cycle checkpoints were not altered in this group of patients.

These observations suggested that these patients, although presenting clinical manifestations similar to those seen in A-T or NBS conditions, clearly differ from these two settings. In addition, the normal DNA-damage sensing, IRIF detection, and IR-induced cell-cycle control indicate that the increased cellular radiosensitivity and γH2AX persistence result from an intrinsic defect in DNA repair.

Defect in the NHEJ Process

In Vivo DNA-Ligation Assay

To analyze the ability of patients' cells to join double-stranded DNA ends by the NHEJ pathway, fibroblasts were transfected with restriction-enzyme-digested, linearized plasmids containing either blunt-blunt or incompatible 3′-3′ overhang ends. Recircularized plasmids were recovered 48 hr after transfection, and their junctions were analyzed by DNA sequencing. The junctions in plasmids recovered from two of the control cell lines (C-1 and C-2) were relatively accurate (71% to 95%), independently of the nature of the DNA-ends (Figures 2A, 2B, and 2C). In striking contrast, in plasmids recovered from the three of the tested patients' cell lines (P1, P2, and P5), the junctions were rarely accurate (0% to 16%), irrespective of the nature of the DNA ends (Figures 2A, 2B, and 2C). These junctions involved various degrees of nucleotide deletion. The mean number of nucleotide loss in inaccurate junctions was significantly higher ($p < 0.001$) in plasmids recovered from patients' cells than in those recovered from controls (Figure 2D).

V(D)J Recombination

Because of its critical dependency on a functional NHEJ machinery, we next analyzed V(D)J recombination in patients fibroblasts upon transfection of the pRecCS extrachromosomal V(D)J recombination substrate and the human full-length lymphoid-specific RAG1- and RAG2-expressing constructs (Nicolas et al., 1998). Coding and signal-join formation, identified by specific PCR amplification of recovered rearranged pRecCS plasmids, was similar or reduced in patients' fibroblasts as compared to control (Figure 3A). Reduced V(D)J recombination activity was further documented in P1 and P2 using an in-chromosome V(D)J assay (Figure S4). Sequence analysis of recovered, rearranged substrates revealed a slight increase in nucleotide loss in coding joins (Figure S3A) compare to controls but not the major alterations typically observed in other NHEJ deficiency situations (Bogue et al., 1997; Rooney et al., 2002; Rooney et al., 2003). In particular, these junctions were not characterized by extensive nucleotide loss or long P nucleotides. In contrast, the fidelity of signal joins was severely impaired in patients' cells. This was first demonstrated by the resistance to ApaII digestion, a restriction-enzyme site created by the perfect fusion of RSS in normal signal joins (Figure 3B). Sequence analysis revealed that 45% of signal joins were imprecise, with nucleotide loss ranging from 6 to 17 bp (Figure S3B). Several sequences suggested the possible usage of microhomology during joining. These V(D)J recombination anomalies are a characteristic feature previously recognized in NHEJ-deficient fibroblasts from Lig4 patients (Badie et al., 1997; Riballo et al., 2001; Buck et al., 2006) and in 2BN cells (Dai et al., 2003).

The V(D)J deficiency in these patients is less severe than in Artemis-deficient RS-SCIDs and probably accounts for the presence of low counts of B and T cells in these patients.

In Vitro NHEJ Assay

Lastly, we analyzed the in vitro end-joining of linearized plasmid DNA by using cell-free extracts (Baumann and West, 1998; Diggle et al., 2003). This DNA-end ligation assay, which results in the formation of DNA concatemers when using control extracts (Figure 3C, lane C), requires a functional NHEJ apparatus, as demonstrated by the absence of DNA oligomers when using extract from a Lig4 deficient patient (L4). Defective DNA multimerization when using extracts from P1-P5 (Figure 3C) strongly argued for a NHEJ defect in these patients. Importantly, the patients' extracts cross-complemented the L4 extract in this assay (Figure 3D), thus eliminating a DNA Lig4 deficiency in P1-P5. Finally, pair-wise mixing of P1-P5 extracts failed to complement the absence of DNA end-joining (Figure 4E), suggesting that the molecular defect may be identical in the five patients.

In conclusion, these data indicated that the five patients present with an identical general DNA-repair defect affecting the NHEJ machinery. This molecular defect translates into an increased cellular sensitivity to DNA-damaging agents in vitro and subsequently into a major failure in the development of both B and T lymphocytes in vivo, thus resulting in a combined immunodeficiency. Although these features are known to be shared by Lig4-deficient patients, a *Lig4* gene defect was excluded in all five of our patients.

(C) BrdU incorporation in proliferating cells and DNA content were analyzed either in untreated or in 5 Gy irradiated cells from a control, an A-T patient, and P1 as a means of analyzing the G1/S cell-cycle checkpoint. While A-T cells did not arrest cycling following IR, P1 cells did.

(D) The fraction of cells in early S phase was determined by FACS analysis with and without 5 Gy IR, as in (C), and was used to calculate the inhibition of S phase entry. A-T and NBS cells were defective in G1/S checkpoints, whereas P1-P5 cells behaved like normal controls.

(E) The phosphorylation of histone H3 and DNA content of either untreated or of 5 Gy-irradiated P1 cells were analyzed by FACS. While A-T cells retained phospho-H3-positive cells following IR, indicating their impaired G2/M checkpoint, P1 cells did not.

(F) The fraction of phospho-H3 positive cells in IR and untreated cells was used to calculate the % inhibition of entry into mitosis in A-T and control cells as well as into cells from P1, P2, and P5. While A-T cells demonstrate a defect in the G2/M checkpoint following IR, patients' cells behaved like normal controls.

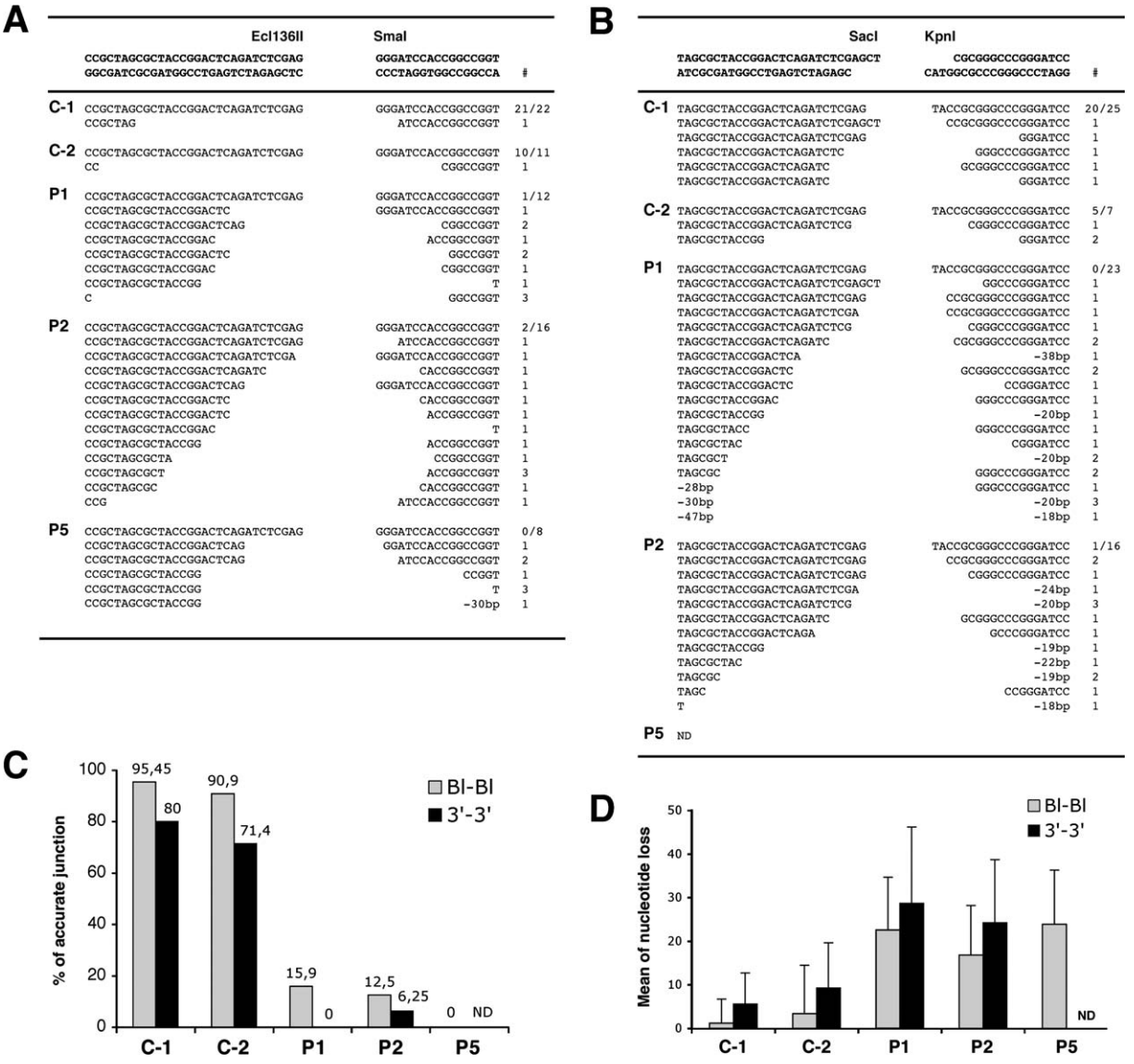

Figure 2. DNA-End Ligation of Linearized Plasmids Is Defective in Patients' Fibroblasts

(A) DNA sequence of junctions was obtained after ligation of blunt-blunt linearized plasmids in fibroblasts from two controls (C-1 and C-2) and patients P1, P2, and P5. The occurrence of a given sequence is indicated on the right.

(B) DNA sequence of junctions was obtained after ligation of 3′-3′ linearized plasmid in fibroblasts from two controls (C-1 and C-2) and patients P1 and P2. The occurrence of a particular sequence is indicated on the right.

(C) Percentages (mean values and standard deviations) of accurate junctions in clones from each set of experiments depicted in (A) and (B). Accurate junctions are defined as the sequences preponderantly shared by the two controls.

(D) Chart representing the mean nucleotide loss in inaccurate junctions observed under the two experimental conditions.

Cloning of *Cernunnos* cDNA

Genetic analysis using highly polymorphic microsatellite markers allowed us to formally exclude a role for the six known NHEJ factor-encoding genes *Ku70, Ku80, DNA-PKcs, Lig4, XRCC4,* and *Artemis* in the four patients (P2-P5) who were born to three consanguineous families since transmission of the disease was independent from the segregation of markers flanking the above-mentioned genes (not shown). We designed a functional complementation cloning strategy based on the rescue of the increased cellular sensitivity to DNA-damaging agents to identify the defective gene. A human thymic cDNA library was introduced into P2 fibroblasts by means of retroviral transduction. Eight separate pools of transduced cells were then treated nine times with the radiomimetic drug bleomycin (0.5 μg/ml) over a period of 88 days. Transduced cDNAs were recovered by PCR amplification of genomic DNA with vector-specific flanking primers. This resulted in discrete bands (from 1

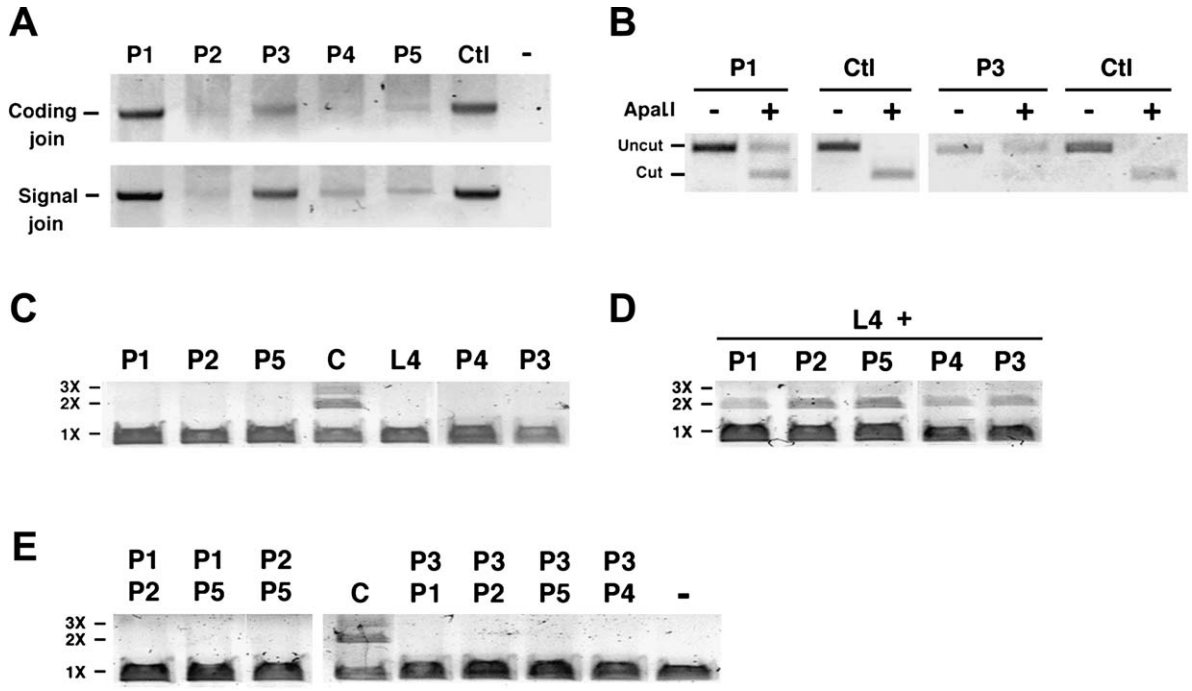

Figure 3. V(D)J Recombination in Fibroblasts and In Vitro NHEJ Are Defective in Patients

(A) SV40-transformed fibroblasts were transfected with RAG1- and RAG2-expressing vectors and the pRecCS extrachromosomal V(D)J recombination substrate. The substrate was recovered 48–72 hr posttransfection, and the formation of signal and coding joins were analyzed by PCR.

(B) The signal-join fidelity was analyzed by ApaII digestion of the PCR products. Signal joins detected in P1 and P3 were imprecise.

(C) Protein extracts from control (C), a Lig4 patient (L4), and P1-P5 cells were incubated with a linearized plasmid. The reaction products were run on agarose gel and stained with SYBR-Green. Multimerized DNA molecules (2× and 3×) were formed with control but not with P1-P5 extracts.

(D) While mixing protein extracts from Lig4 (L4) together with P1-P5 cells eliminated the NHEJ defect, using either one independently resulted in the emergence of the defect, indicating that P1-P5 defect is not Lig4.

(E) Pair-wise mixing of P1-P5 cellular extracts failed to complement the patient's NHEJ defect, suggesting that P1-P5 belong to the same complementation group.

to 6) in all eight pools of transduced cells (data not shown), which suggested a specific outgrowth of cells that had received a cDNA complementing their endogenous gene defect. DNA sequencing identified an identical cDNA present in the PCR products from seven of the pools.

This cDNA (EMBL:AJ972687) covers 2063 nucleotides and encodes a hypothetical protein of 299 amino acids (aa), which we named Cernunnos (Figure 4A). The *Cernunnos* gene (GeneID: 79840), located on human chromosome 2q35, is composed of eight exons with sizes ranging from 59 bp to 1130 bp (Figure 4B). The *Cernunnos* gene has never been described previously (except for the in silico-derived hypothetical protein FLJ12610), and database searching did not disclose any obvious homology with other known proteins or functional domains. cDNA cloning of the murine *Cernunnos* counterpart revealed a 74% protein identity over the whole sequence, suggesting a high degree of conservation among higher eukaryotes (not shown). RT-PCR analysis of a panel of 15 cDNAs representing a wide range of human tissues demonstrated that *Cernunnos* is ubiquitously expressed (Figure 4C). Finally, immunofluorescence analysis of ectopically expressed, V5 epitope-tagged Cernunnos in fibroblasts revealed a predominant nuclear localization (Figure 4D). These last two findings are compatible with Cernunnos being a general DNA repair factor.

Cernunnos Mutations

Mutations affecting the *Cernunnos* encoding gene were identified in all five patients (Figure 4B). P1 carries two missense heterozygous mutations, C259G (cDNA) in exon 2 and T457C in exon 3, leading to R57G and C123R aa substitutions respectively. P2 displays a homozygous C622T nonsense mutation in exon 5, changing an arginine codon at position 178 to a stop codon (R178X), thus resulting in a putative protein lacking about one-third of the C terminus region. P3 and P4 carry a homozygous deletion of G267, the last nucleotide of exon 2, as well as a homozygous A to T change three nucleotides downstream in intron 2 (Figure 4B). These two associated mutations result in a mixed RNA population. Normally spliced RNAs carry the G267 deletion, resulting in a frameshift at K69 followed by a premature stop codon, while numerous aberrant splicing events lead to severely truncated putative proteins. Of note, one of these mutated forms may retain some activity as it presents an internal in-frame deletion covering A25-R57 (data not shown). Lastly, P5 carries a homozygous C259G substitution in exon

A

```
 GGCCTCTTACTCTAGGCCTTTCGGTTTGCGCGAGCGGGCAGGAAAGCGTGCGTGCGGCTAAGAGAGTGGGCGCTCTCGCGGCCGCTGACG      90
ATG GAA GAA CTG GAG CAA GGC CTG TTG ATG CAG CCA TGG GCG TGG CTA CAG CTT GCA GAG AAC TCC CTC     159
 M   E   E   L   E   Q   G   L   L   M   Q   P   W   A   W   L   Q   L   A   E   N   S   L      23

TTG GCC AAG GTT TTT ATC ACC AAG CAG GGC TAT GCC TTG TTG GTT TCA GAT CTT CAA CAG GTG TGG CAT     228
 L   A   K   V   F   I   T   K   Q   G   Y   A   L   L   V   S   D   L   Q   Q   V   W   H      46

GAA CAG GTG GAC ACT AGT GTG GTC AGC CAG CGA GCC AAG GAG CTG AAC AAG CGG CTC ACT GCT CCT CCT     297
 E   Q   V   D   T   S   V   V   S   Q   R   A   K   E   L   N   K   R   L   T   A   P   P      69

GCA GCT TTC CTC TGT CAT TTG GAT AAT CTC CTT CGC CCA TTG TTG AAG GAC GCT GCT CAC CCT AGC GAA     366
 A   A   F   L   C   H   L   D   N   L   L   R   P   L   L   K   D   A   A   H   P   S   E      92

GCT ACC TTC TCC TGT GAT TGT GTG GCA GAT GCA CTG ATT CTA CGG GTG CGA AGT GAG CTC TCT GGC CTC     435
 A   T   F   S   C   D   C   V   A   D   A   L   I   L   R   V   R   S   E   L   S   G   L     115

CCC TTC TAT TGG AAT TTC CAC TGC ATG CTA GCT AGT CCT TCC CTG GTC TCC CAA CAT TTG ATT CGT CCT     504
 P   F   Y   W   N   F   H   C   M   L   A   S   P   S   L   V   S   Q   H   L   I   R   P     138

CTG ATG GGC ATG AGT CTG GCA TTA CAG TGC CAA GTG AGG GAG CTA GCA ACG TTA CTT CAT ATG AAA GAC     573
 L   M   G   M   S   L   A   L   Q   C   Q   V   R   E   L   A   T   L   L   H   M   K   D     161

CTA GAG ATC CAA GAC TAC CAG GAG AGT GGG GCT ACG CTG ATT CGA GAT CGA TTG AAG ACA GAA CCA TTT     642
 L   E   I   Q   D   Y   Q   E   S   G   A   T   L   I   R   D   R   L   K   T   E   P   F     184

GAA GAA AAT TCC TTC TTG GAA CAA TTT ATG ATA GAG AAA CTG CCA GAG GCA TGC AGC ATT GGT GAT GGA     711
 E   E   N   S   F   L   E   Q   F   M   I   E   K   L   P   E   A   C   S   I   G   D   G     207

AAG CCC TTT GTC ATG AAT CTG CAG GAT CTG TAT ATG GCA GTC ACC ACA CAA GAG GTC CAA GTG GGA CAG     780
 K   P   F   V   M   N   L   Q   D   L   Y   M   A   V   T   T   Q   E   V   Q   V   G   Q     230

AAG CAT CAA GGC GCT GGA GAT CCT CAT ACC TCA AAC AGT GCT TCC CTG CAA GGA ATC GAT AGC CAA TGT     849
 K   H   Q   G   A   G   D   P   H   T   S   N   S   A   S   L   Q   G   I   D   S   Q   C     253

GTA AAC CAG CCA GAA CAA CTG GTC TCC TCA GCC CCA ACC CTC TCA GCA CCT GAG AAA GAG TCC ACG GGT     918
 V   N   Q   P   E   Q   L   V   S   S   A   P   T   L   S   A   P   E   K   E   S   T   G     276

ACT TCA GGC CCT CTG CAG AGA CCT CAG CTG TCA AAG GTC AAG AGG AAG AAG CCA AGG GGT CTC TTC AGT     987
 T   S   G   P   L   Q   R   P   Q   L   S   K   V   K   R   K   K   P   R   G   L   F   S     299

TAA TCTGTTGTGGCCTCAGCTGCTGAGGATGGACTTGGAGAACAGCTTCCAAGCTTCACCTTGAAAGAAGCTTACATGGCAGCAATATTT    1077
 *
CTAAAATAGTGATACAGTCAGAGGCCTCCTGTAAGGGCGAGAGAACTGAAGTTGATGTTGACAGGCCCACAGGGAATTGGCCTTCCCTGTT    1168
CAAGTGGAAGCCAGTCTCTGAGAATCCCGTGCTCTCCTCTCTTTTGGTGGAGGTTCTGTAGGTTCAGGTTTCTACCATGGACTTTAGGTAT    1259
ATAGGGCAAGTCAGCAAGAAAGCACCACACACTCAGGAAGCCTTGTCTACCTTTCCCTAGCGTCTCTAGCCAGCCAGCCCCAGATACTCCT    1350
CAGAGACCCACTTCTCTCTTTTGCATGGAATAAAAAGCACTCACAGTCCCTGCTTTTGGGATTACTTATGCTGTGGAACTCATAACCCAAT    1441
TCACTTCCTTCACTGGGTCCCACCCCATTGTTGTCTCTGGATGAAGTCTAGCCATCAGTCTGGTCCTTCAGATTCTTCGTAAACTTTTCTG    1532
CAGTTGCCAGAGCTAAGTCTCCATTTGGAAACTTTGATCTCAAGAACTCTCTTGATGGTGGGCACAAGACAGATAGGTGATTGCTGCTTTC    1623
CTTTGCCAAACTTGGATGCATTTTTCTCTTTGTTTCCAAAGTATAGGCAACAGGTTAAACTACCACGTGGGGTAGTTTATCAATCCTCCCG    1714
CCTCATCCTTCTGCATAACTGGGACTAAAGGCACACACCACCACACCTAGCTAATTTTTGTATTTTTTTGTGTGTGGAGACAAGGCTTTGC    1805
CATGTTGCCCAGGCTGGTCTTGAACTCCTGGACTCTAGTGATCTGCCCACCTCAACCTCCCAAAGTGCTGGGATTACAGGCATGAGCTACC    1896
ACGCCTATCCAATTTCTGGTTTATTTACTTTCGATGGTTAAATGCCTCCTTATTCAAATATCCTGTATATATACTGGCGTTTCTGTCCTGA    1987
TGTCAAGTCTCGAGAGAAGATGATCAAACAATAATAAAATAATTATAATAAGAACAACAAAAAAAAAAAAAAAAAA                    2063
```

B

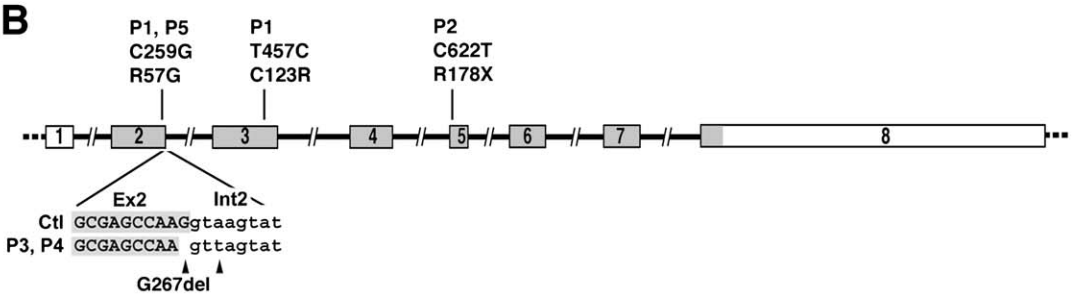

C

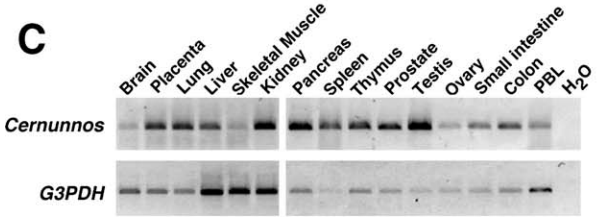

D

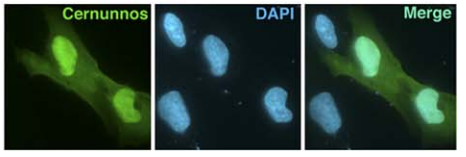

2, resulting in R57G aa modification. We confirmed the autosomal recessive inheritance of the identified mutations by sequencing parents' DNA in all cases (data not shown).

Complementation of the NHEJ Defect by wt *Cernunnos*

We next evaluated the complementation of the NHEJ defect by ectopic expression of *wt Cernunnos*. Primary fibroblasts from P1, P2, and P3 were transduced with a bicistronic Cernunnos-ires-GFP retrovirus, resulting in 86%, 75%, and 80% GFP-positive cells respectively. The survival curves of these transduced cells after ionizing radiation (0, 1, and 3 Gy) indicated a return to an overall normal radiosensitivity as compared to control cells (Figure 5A). Likewise, the V(D)J recombination was fully restored upon transfection of wt *Cernunnos,* as demonstrated by the complete ApaII digestion of PCR-amplified signal joins (Figure 5B) and in-chromosome V(D)J assay (Figure S4). Lastly, cell-free extracts from *Cernunnos*-transfected fibroblasts were able to oligomerize linear DNA molecules in the in vitro NHEJ assay (Figure 5C). Taken together, these results confirm that the identified *Cernunnos* mutations are responsible for the defective DNA repair in this series of patients.

DISCUSSION

T and B Cell Combined Immunodeficiency, Microcephaly, and Growth Retardation Caused by *Cernunnos* Mutations

We herein describe a T and B cell combined immunodeficiency characterized by a progressive lymphocytopenia associated with developmental defects including microcephaly as well as growth retardation and an increased cellular sensitivity to IR. This new rare human autosomal recessive primary immunodeficiency is caused by deleterious mutations in a novel general DNA repair factor we have named Cernunnos. The independent identification of the same factor, named XLF, is reported by Ahnesorg et al. in another article in this issue of *Cell* (Ahnesorg et al., 2006). Strikingly, the clinical phenotype of Cernunnos-deficient patients shares several characteristics with Nijmegen breakage syndrome and Lig4 deficiency. However, Cernunnos deficiency does not lead to impaired cell-cycle checkpoints, as observed in NBS condition, but leads rather to an NHEJ defect as observed in Lig4 deficiency as well as in the 2BN patient (Carney et al., 1998; Matsuura et al., 1998; Varon et al., 1998; Dai et al., 2003; Buck et al., 2006).

DSB are introduced in DNA during the V(D)J recombination process. A complete failure to resolve these breaks leads to an arrest in B and T cell development, as observed in Artemis-deficient RS-SCID condition and in the respective animal models (Revy et al., 2005). A residual DNA end-joining activity, as observed in the case of hypomorphic Lig4 and Artemis mutations, allows for limited development of B and T cells (Moshous et al., 2003; Smith et al., 2003). The partially compromised (around 10% of normal value as shown in Figure S4C) V(D)J recombination identified in Cernunnos-deficient fibroblasts is comparable to that of hypomorphic Lig4-deficient cells and may account for the severe T and B cell lymphopenia observed in Cernunnos deficiency. The low counts of circulating T and B cells may in fact reflect a residual Cernunnos activity caused by hypomorphic mutations. The nature of the different mutations identified in the patients is compatible with expression of a Cernunnos protein, albeit truncated in some cases (P2-P4). In Cernunnos patients, the presence of memory-only T cells in combination with the progressive loss of B lymphocytes suggest that while a wave of lymphocyte production did occur at some point, the sustained renewal of the immune system is profoundly impaired in these patients. These observations, taken together with our observation of the occurrence of bone marrow aplasia in P5, suggest that the Cernunnos defect may be associated with a compromised haemo-/lymphopoiesis. T cell lymphopenia appears relatively milder as compared to B cell, at least in the eldest patients. Expansion of long-lived memory T cells as observed in other combined T+B immunodeficiencies caused by other hypomorphic gene mutations (DiSanto et al., 1994; Moshous et al., 2003; De Villartay et al., 2005) can account for this observation.

Although patients displayed a hypogamaglobulinemia, the levels of serum IgM (Table 1) were occasionally as high as observed in classical CSR-deficient hyper-IgM syndromes (Durandy et al., 2005). This suggests a possible role for Cernunnos in CSR. Autoimmunity is another consequence of the immunodeficiency caused by Cernunnos deficiency, as also observed in other combined T+B cell immunodeficiencies caused by hypomorphic mutation of RAG1 (De Villartay et al., 2005). It may result from a skewed T cell repertoire subsequent to partially defective T+B development or to defective peripheral control of response to self antigens.

Beside the patent immunological consequences of Cernunnos deficiency, developmental defects, notably microcephaly, are also present. This is reminiscent of the microcephaly that has been noted in some Lig4-deficient patients (Riballo et al., 1999; O'Driscoll et al., 2001; Buck et al., 2006), as well as of the embryonic lethality of Lig4 (and XRCC4) KO mice due to massive apoptosis of postmitotic neurons (Barnes et al., 1998; Frank et al., 1998; Gao et al., 1998). This suggests that Cernunnos plays a role in the development of the central nervous system. Indeed, proficient DNA-damage responses, including NHEJ and HR, have been shown to be essential during the development

Figure 4. *Cernunnos:* cDNA Sequence, Genomic Organization, Patients' Mutations, cDNA Expression, and Subcellular Localization

(A) *Cernunnos* cDNA sequence and protein (1-letter code).

(B) *Cernunnos* gene organization with the mutations identified in patients. Gray regions represent the coding sequence.

(C) RT-PCR analysis using a panel of cDNA from 15 different human tissues. G3PDH-specific primers were used as control.

(D) Nuclear localization of transfected V5-epitope-tagged Cernunnos in fibroblasts determined by immunofluorescence.

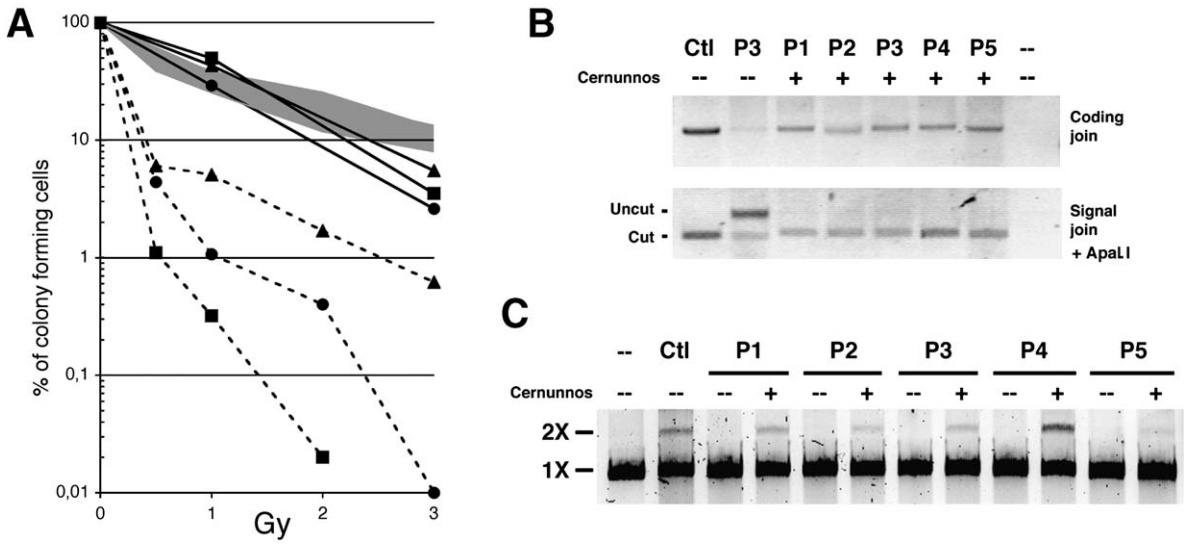

Figure 5. Complementation of the DNA-Repair Defect by wt Cernunnos

(A) Primary fibroblasts from P1 (squares), P2 (circles), and P3 (triangles) were transduced with Cernunnos-iresGFP retrovirus and exposed to ionizing radiation (solid lines), and their survival compared to untransduced cells (dash lines) and normal control cells (gray envelope).

(B) V(D)J recombination coding join-formation and signal join-fidelity (complete ApaII digestion) were restored by wt Cernunnos in P1-P5 fibroblasts.

(C) Wt Cernunnos complemented the in vitro NHEJ defect in cellular extracts from transfected P1-P5 cells.

of the brain (Abner and McKinnon, 2004). Whether Cernunnos, comparably to Lig4/XRCC4, is an essential factor for viability is currently unknown. The development of a Cernunnos KO mouse is likely to assist in clarifying this issue.

NHEJ factors are considered genomic caretakers since they guarantee genomic integrity through the proper repair of DNA lesions (Ferguson and Alt, 2001; Dudley et al., 2005; Revy et al., 2005). Indeed, analysis of several animal models has indicated that NHEJ deficiency may result in chromosomal aberrations such as translocations or telomeric fusions, the consequence of which is a high propensity to develop cancer. In the immune system, the introduction of an NHEJ defect into a P53 mutated background invariably leads to the development of pro-B cell lymphomas in mice (Ferguson and Alt, 2001). Likewise, hypomorphic mutations in *Lig4* and *Artemis* in humans have been found to be associated with the onset of lymphopoietic malignancies (Riballo et al., 1999; Moshous et al., 2003). The question of the genomic caretaker status of Cernunnos is of importance because it may turn out that Cernunnos deficiencies are linked to a higher risk of developing cancer. The implication of Cernunnos in NHEJ in combination with the fact that two Cernunnos deficient patients (P1 and P5) exhibited several chromosome alterations support this assumption. The analysis of Cernunnos KO mice will help to clarify this important issue.

What Is the Role for Cernunnos in NHEJ?

The in vitro NHEJ assay clearly identified Cernunnos as a key constituent of the DNA end-joining reaction. The remarkable parallel in the clinical/biological presentations of Cernunnos with Lig4 deficiencies strongly suggests that Cernunnos could be a third partner in the XRCC4/Lig4 complex. Indeed, the accompanying article from Stephen Jackson's laboratory reports on the identification of the same factor (named XLF) through two-hybrid screen using XRCC4. Moreover, the interaction of Cernunnos/XLF with the XRCC4:DNA-LigaseIV complex in vivo was further documented through coimmunoprecipitation experiments (Ahnesorg et al., 2006 and unpublished data). Several biochemical and genetic studies in yeast and mammals have previously identified XRCC4 and/or Lig4 interacting factors. Among those, Nej1/Lif2p has been described only in *S. cerevisae* (Frank-Vaillant and Marcand, 2001; Kegel et al., 2001; Ooi et al., 2001; Valencia et al., 2001). Nej1 interacts with the yeast XRCC4 homolog (Lif1) and is critically required for NHEJ. Moreover, Nej1 is specifically repressed during mating type-switching in yeast, a DNA recombination process that relies exclusively on homologous recombination. No homologs for Nej1 have yet been identified in higher eukaryotes. Further studies are now required to determine whether or not Cernunnos represents a functional, although highly divergent, homolog of Nej1 in mammals.

EXPERIMENTAL PROCEDURES

Patients

The patients' clinical phenotypes are shown in Table 1.

Five patients from four families (including three consanguineous families) were included. P3 and P4 were siblings. Family history revealed that three older sisters of P2 died from severe infections during their first year of life. All patients presented with growth retardation (-3SD), already existent at birth in two of them, or during the first year of life in the other three. Microcephaly (-3SD) at birth was a constant feature in all patients. Facial dysmorphia was mild in P1 but was more prominent in P3-P4 and P5, who presented with a birdlike face. Bone malformations were present in P1 (i.e., low implantation of the thumb) and in P3-P4 (i.e., hypoplasia of

the middle phalanx of the fifth finger). Malformations of the kidney (i.e., nephroptosis) and of the genital organs were also present in P1. Mental retardation was evident only in P1. P5 suffered from bone-marrow aplasia, which was first diagnosed at the age of one year. Chromosomal analyses revealed a normal 46XY karyotype but several spontaneous, nonrecurrent, chromosomal translocations in patients P1 and P5 lymphocytes.

All patients experienced severe infections; P1 developed recurrent bacterial infections of the respiratory tract beginning at the age of three years and invasive warts and a life-threatening cholangitis which had been diagnosed at eight years of age. P2 suffered from recurrent bacterial infections of the respiratory and digestive tracts from the first months of life onward. P3 presented with a *Pneumocystis carinii* pneumonia, chronic *Giardia lamblia* enteritis, and *Salmonella* and *Campylobacter* enteritis as well as molluscum contagiosum and warts from three years of age onward. His sister, P4, had neonatal pneumonia and suffered from mild recurrent infections of the upper respiratory tract. P5 developed bacterial infections of the respiratory tract from the first year of life onward. Two patients (P1 and P3) also developed autoimmune manifestations—hemolytic anemia at four years of age and thrombocytopenia at eight years of age, respectively. P1 received immunosuppressive therapy over a five-year period and was finally splenectomized. As soon as lymphopenia and hypogammaglobulinemia were diagnosed, patients were started on immunoglobulin substitution. Although under treatment, P1 and P2 both died from a septic shock. P3, P4, and P5 currently remain alive, supported by immunoglobulin substitution and antibiotic prophylaxis (in P3 and P4). In accordance with the Helsinki Declaration, informed consent for our study was obtained from the families. This study was also approved by the (INSERM) Institutional Review Board. Primary skin fibroblasts were obtained from skin biopsies of all five patients as well as RS-SCID, Lig4, Ataxia telangiectasia, Nijmegen breakage syndrome patients in addition to normal controls. SV40-transformed and telomerase-immortalized cell lines were obtained as described (Nicolas et al., 1998; Poinsignon et al., 2004).

Antibodies

Rabbit polyclonal anti-phospho-histone H3 and anti-phospho-H2A-X (Ser139) came from Upstate (Lake Placid, NY). Mouse monoclonal antibodies directed against MRE11 (clone 12D7) and RAD51 (clone 14B4) originated from Abcam (Cambridge, UK). Alexa-568 and Alexa-488 goat-F(Ab′)$_2$ secondary antibodies were from Molecular probes (Eugen, OR). FITC-conjugated anti-BrdU antibody and goat F(Ab′)$_2$ anti-rabbit immunoglobulin G were purchased from Becton Dickinson (Mountain View, CA). Mouse monoclonal anti-V5 antibody came from Invitrogen.

IR Sensitivity Assay

IR sensitivity was analyzed by clonogenic assays upon γ rays exposure of primary fibroblasts, as previously described (Nicolas et al., 1998). For IR sensitivity complementation analysis, primary fibroblasts were transduced using a bicistronic Cernunnos-iresGFP-expressing retrovirus and subjected to various doses of γ rays (0, 1, 3 Gy).

Immunofluorescence Detection of IRIFs

Primary fibroblasts were seeded on cover slips and X-irradiated (Faxitron-160FW, EDIMEX, Wheeling, IL; 10 Gy; 166 rad/min). Two hours after irradiation, cells were washed with PBS and fixed with 4% paraformaldehyde in PBS for 15 min. After each step, the cover slips were rinsed three times with PBS. Cells were incubated for 20 min with PBS containing 0.1M glycine and permeabilized in 0.5% Triton X-100 in PBS for 15 min. Cells were incubated for 30 min with the PBS-BSA solution. Cells were then labeled with the appropriate primary antibodies, followed by washes with PBS-BSA solution and incubation with secondary antibodies. Slides were counterstained with 0.1 μg/ml of DAPI (4′, 6′-diamidino-2-phenylindole) and mounted in Fluorsave (Calbiochem). Slides were viewed by epifluorescence microscopy (Axioplan ZEISS), and images were taken by a cooled charge-coupled device (CCD) camera. Grayscale images were processed using Adobe Photoshop 5.5. (San Jose, CA).

γH2AX Detection by Fluorocytometry

Fibroblasts were incubated at 37ºC with medium alone or containing 10 μg/ml of Bleomycin (Aventis) for 1 hr and then washed and incubated in complete medium. Thirty minutes or 24 hr later, cells were harvested and fixed in ethanol 70%. Permeabilization was performed with 0.1% triton X-100 and 4% FBS. Cells were resuspended with anti-γH2AX antibody (dilution 1:500) and incubated for 2 hr. Cells were washed and resuspended with a 1:1000 dilution of goat anti-mouse IgG (Alexa 488) for 1 hr. Samples were washed and analyzed by a Becton Dickinson FACScan flowcytometer.

Cell-Cycle Analysis

G1/S checkpoint analysis was performed as previously described (Moshous et al., 2003). For G2/M checkpoint analysis, 3×10^5 immortalized SV40-transformed fibroblasts were harvested 1 hr after 5 Gy X-irradiation, washed with PBS, fixed with cold 70% ethanol, and kept at –20ºC for 16 hr. After washing, the cells were resuspended in PBS 0.25% with Triton X-100 and incubated on ice for 15 min. Cells were washed in PBS and incubated with 1 μg of anti-phospho-H3 in PBS-1% BSA for 3 hr. Anti-P-H3 was detected with FITC-conjugated F(Ab′)$_2$ goat anti-rabbit IgG antibody. The cells were washed and resuspended in PBS containing 25 μg/ml PI. Fluorescence was measured by using a Becton Dickinson FACScan flowcytometer. For RDS assay, primary fibroblasts were pulse-labeled for 2 hr with 10 μl of [^{3}H]thymidine (1.5 MBq/ml) 45 min following 0 to 40 Gy IR exposure.

In Vivo Plasmid Religation Assay

Five μg of a modified version of EGFP-N2 plasmid (Clontech) were linearized by either SacI and KpnI in order to generate 3′-3′ ends or by EcI136II and SmaI in order to generate blunt endsand introduced into SV40-transformed fibroblasts by electroporation. Recircularized plasmids were recovered by hirt lysis 48 hr after transfection, and the junctions were PCR-amplified using primers CMV 5′-CGTGTACGGTGGGAGGTC-3′ and GFPr 5′-CGGACACGCTGAACTTGTGG-5′. PCR products were cloned in pGemT (Promega) and sequenced.

V(D)J Recombination Assay

V(D)J recombination on extra chromosomal substrates was performed as previously described using full-length human Rag1 and Rag2 (Nicolas et al., 1998; Moshous et al., 2001). The pRecCS V(D)J recombination reporter substrate has RSS in an orientation which drives V(D)J recombination by inversion, thus retaining both coding and signal joins, these then being PCR-amplified using specific combinations of primers. For complementation analysis in fibroblasts, 2.5 μg of wt*Cernunnos* cloned in pCDNA3.1D (Invitrogen) was cotransfected. V(D)J recombination assay on chromosome integrated substrate was performed as previously described (Poinsignon et al., 2004).

In Vitro NHEJ Assay

Whole-cell extracts (WCE) preparation and in vitro NHEJ assay were performed using a procedure adapted from Baumann et al. and Diggle et al. (Baumann and West, 1998; Diggle et al., 2003). Briefly, after washing in 1× PBS, cells were lysed through three freeze/thaw cycles in LB buffer (25 mM Tris [pH 7.5], 333 mM KCl, 1.3 mM EDTA, 4 mM DTT, protease and phosphatase inhibitors). Lysates were incubated for 20 min at 4ºC and cleared by centrifugation. Supernatants were dialyzed against 1× E buffer (20 mM Tris [pH 8.0], 20% glycerol, 0.1 M K(OAc), 0.5 mM EDTA, 1 mM DTT). WCE were adjusted to 5 μg/μl and kept frozen (−80ºC) until use. For NHEJ assay, 15 μg of WCE was incubated (10 μl reaction) with 25 ng of linear DNA (EcoRI digested pEGFPN2) in 1× LigB (250 mM Tris [pH 8.0], 300 mM K(OAc), 2.5 mM Mg(OAc)2, 5 mM ATP, 5 mM DTT, 0.5 mg/ml BSA, 1 μg/ml IP6) for 2 hr at 37ºC. Reactions were then treated with 1 μl RNase (1 mg/ml) for 5 min at RT and with 2 μl of 5× deproteination solution (10 mg/ml Proteinase K, 2.5% SDS, 50 mM EDTA, 100 mM Tris [pH 7.5]) for 30 min at 55ºC. After migration of the samples in 0.7% agarose, the gels were stained with SYBR-Green (30 min), and fluorescence was detected via a FluorImager.

cDNA Complementation Cloning

SV40-transformed, telomerase-immortalized fibroblasts from P2 were transduced with a commercially available human thymic cDNA library cloned into the pFB retroviral vector (ViraPort XR Plasmid Human Thymus cDNA library, Stratagene) as described (Moshous et al., 2003). Transduced cells were kept in culture for 88 days. During this time period, they were treated nine times with bleomycin (0.5 μg/ml in RPMI for 1 hr). cDNA inserts were recovered from genomic DNA by PCR-amplification using vector-specific primers FBP1 (5′-CCTCAAAGTAGACGGCATCGC AGCTTGGAT-3′) and FBP2 (5′-CGAACCCCAGAGTCCCGCTCAGAAGA ACT-3′). PCR bands were gel-purified and directly sequenced using FBP1 and subsequent internal primers. The Cernunnos ORF was PCR-amplified (F1 CACCTCGCCACATGGAAGAACTGGAGCAA, R1 ACTGAAGAGACC CCTTGCCCTTCTTCC) and cloned with a C terminus V5-epitope/6xHis tag in pCDNA3.1D (Invitrogen) and a C terminus myc-epitope/6xHis tag in the retroviral vector pMND-MFG (Robbins et al., 1998). The genomic organization of *Cernunnos* gene was determined in silico through Blast analysis of the cDNA against human genomic sequences.

Cernunnos Gene Sequencing and Expression Analysis

The eight exons of *Cernunnos* were PCR-amplified by using genomic DNA and Taq High Fidelity polymerase (Roche Diagnostics, Mannheim, Germany) in addition to the following oligonucleotide primer pairs: 1F 5′-CCGCCCACGCCAGGCATAGG-3′, 1R 5′-GGCTTCGTCGCACCAAACA GG-3′; 2F 5′-GTTGATACAGACTGGTTTGG-3′, 2R 5′-TCAACCCGATTC AACCTTCC-3′; 3F 5′-TTGCCTTCGTGTTAACCAGG-3′, 3R 5′-CTAAAG CTTCCTCTCAAAGC-3′; 4F 5′-ATGTAAATGGGTTACTTGCC-3′, 4R 5′-GTTTCTGGTTAGTATTCAGC-3′; 5F 5′-CCTCCTCTTTCCTAAGTAGC-3′, 5R 5′-AGACAAAGGGCATTCCAACC-3′; 6F 5′-CCCCTATTGGATCT AACTGC-3′, 6R 5′-TCATATTGGACAGCATAAACC-3′; 7F 5′-TATTTGTA CCAAACCCTGG-3′, 7R 5′-GCAATTCCAGGGACCACTGG-3′; 8F 5′-CATGAGAGGAAGAAAGTTCC-3′, 8R 5′-ATTCTCAGAGACTGGCTT CC-3′. RT-PCRs were performed with primers Cernunnos-F 5′-TTTCGGT TCGCGCGAGCGGG-3′ and Cernunnos-R 5′-CACTATTTTAGAAATATT GC-3′. All PCR products were directly sequenced. PCR-ready cDNAs from several tissues (Clontech) were amplified with primers Cernu-F 5′-TTGATTCGTCCTCTGATGGG-3′ and Cernunnos-R or G3PDH primers. They were then run onto 1% agarose gels, and bands were stained with ethidium bromide.

Supplemental Data

Supplemental Data include four figures and can be found with this article online at http://www.cell.com/cgi/content/full/124/2/287/DC1/.

ACKNOWLEDGMENTS

We are indebted to Dr. Irene Ward for the kind gift of the mouse monoclonal anti-53BP1 antibody and to Dr. Tobias Ankermann for blood and fibroblast samples from P3 and P4. We acknowledge Monique Forveille for her technical assistance. We thank Dr. Sylvain Latour for discussions and critical reading of the manuscript. We acknowledge Drs. I. Tezcan and F. Ersoy for their contribution to the followup of the patient P2. This work was supported by institutional grants from INSERM as well as grants from the Association de Recherche sur le Cancer (ARC), the Ligue National contre le Cancer (Equipe labelisée LA LIGUE 2005, EL2005.LNCC/JPDV1), the Commissariat à l'Energie Atomique (LRC-CEA N°40V), the French Rare Disease Program (GIS), the INCa/Cancéropôle IdF, and the Euro-Policy-PID (n°PL 006411). P.R. is a scientist from the Centre National de la Recherche Scientifique (CNRS). D.B. received fellowships from the European Academy of Allergy and Clinical Immunology (EAACI), the Association pour la Recherche sur le Cancer (ARC), and the City of Paris.

Received: October 3, 2005
Revised: November 22, 2005
Accepted: December 14, 2005
Published: January 26, 2006

REFERENCES

Abner, C.W., and McKinnon, P.J. (2004). The DNA double-strand break response in the nervous system. DNA Repair (Amst.) *3*, 1141–1147.

Ahnesorg, P., Smith, P., and Jackson, S.P. (2006). XLF interacts with the XRCC4-DNA ligase IV complex to promote DNA nonhomologous end-joining. Cell *124*, this issue, 301–313.

Badie, C., Goodhardt, M., Waugh, A., Doyen, N., Foray, N., Calsou, P., Singleton, B., Gell, D., Salles, B., Jeggo, P., et al. (1997). A DNA double-strand break defective fibroblast cell line (180BR) derived from a radiosensitive patient represents a new mutant phenotype. Cancer Res. *57*, 4600–4607.

Barnes, D.E., Stamp, G., Rosewell, I., Denzel, A., and Lindahl, T. (1998). Targeted disruption of the gene encoding DNA ligase IV leads to lethality in embryonic mice. Curr. Biol. *8*, 1395–1398.

Bassing, C.H., and Alt, F.W. (2004). H2AX may function as an anchor to hold broken chromosomal DNA ends in close proximity. Cell Cycle *3*, 149–153.

Bassing, C.H., Swat, W., and Alt, F.W. (2002). The mechanism and regulation of chromosomal V(D)J recombination. Cell *109 Suppl*, S45–S55.

Baumann, P., and West, S.C. (1998). DNA end-joining catalyzed by human cell-free extracts. Proc. Natl. Acad. Sci. USA *95*, 14066–14070.

Bogue, M.A., Wang, C., Zhu, C., and Roth, D.B. (1997). V(D)J recombination in Ku86-deficient mice: distinct effects on coding, signal, and hybrid joint formation. Immunity *7*, 37–47.

Buck, D., Moshous, D., de Chasseval, R., Ma, Y., Le Deist, F., Cavazzana-Calvo, M., Fischer, A., Casanova, J.L., Lieber, M.R., and De Villartay, J.P. (2006). Severe combined immunodeficiency and microcephaly in siblings with hypomorphic mutations in DNA ligase IV. Eur. J. Immunol. *36*, 224–235.

Carney, J.P., Maser, R.S., Olivares, H., Davis, E.M., Le Beau, M., Yates, J.R., 3rd, Hays, L., Morgan, W.F., and Petrini, J.H. (1998). The hMre11/hRad50 protein complex and Nijmegen breakage syndrome: linkage of double-strand break repair to the cellular DNA damage response. Cell *93*, 477–486.

Dai, Y., Kysela, B., Hanakahi, L.A., Manolis, K., Riballo, E., Stumm, M., Harville, T.O., West, S.C., Oettinger, M.A., and Jeggo, P.A. (2003). Nonhomologous end joining and V(D)J recombination require an additional factor. Proc. Natl. Acad. Sci. USA *100*, 2462–2467.

de Villartay, J.P., Fischer, A., and Durandy, A. (2003). The mechanisms of immune diversification and their disorders. Nat. Rev. Immunol. *3*, 962–972.

De Villartay, J.P., Lim, A., Al-Mousa, H., Dupont, S., Déchanet-Merville, J., Caumau-Gatbois, E., Gougeon, M.L., Lemainque, A., Eidenschenk, C., Jouanguy, E., et al. (2005). A novel immunodeficiency associated with hypomorphic RAG1 mutations and CMV infection. J. Clin. Invest. *115*, 3291–3299.

Diggle, C.P., Bentley, J., and Kiltie, A.E. (2003). Development of a rapid, small-scale DNA repair assay for use on clinical samples. Nucleic Acids Res. *31*, e83.

DiSanto, J.P., Rieux-Laucat, F., Dautry-Varsat, A., Fischer, A., and de Saint Basile, G. (1994). Defective human interleukin 2 receptor gamma chain in an atypical X chromosome-linked severe combined immunodeficiency with peripheral T cells. Proc. Natl. Acad. Sci. USA *91*, 9466–9470.

Dudley, D.D., Chaudhuri, J., Bassing, C.H., and Alt, F.W. (2005). Mechanism and control of V(D)J recombination versus class switch recombination: similarities and differences. Adv. Immunol. *86*, 43–112.

Durandy, A., Revy, P., Imai, K., and Fischer, A. (2005). Hyper-immunoglobulin M syndromes caused by intrinsic B-lymphocyte defects. Immunol. Rev. *203*, 67–79.

Dynan, W.S., and Yoo, S. (1998). Interaction of Ku protein and DNA-dependent protein kinase catalytic subunit with nucleic acids. Nucleic Acids Res. *26*, 1551–1559.

Ferguson, D.O., and Alt, F.W. (2001). DNA double strand break repair and chromosomal translocation: lessons from animal models. Oncogene *20*, 5572–5579.

Frank, K.M., Sekiguchi, J.M., Seidl, K.J., Swat, W., Rathbun, G.A., Cheng, H.L., Davidson, L., Kangaloo, L., and Alt, F.W. (1998). Late embryonic lethality and impaired V(D)J recombination in mice lacking DNA ligase IV. Nature *396*, 173–177.

Frank-Vaillant, M., and Marcand, S. (2001). NHEJ regulation by mating type is exercised through a novel protein, Lif2p, essential to the ligase IV pathway. Genes Dev. *15*, 3005–3012.

Gao, Y., Sun, Y., Frank, K.M., Dikkes, P., Fujiwara, Y., Seidl, K.J., Sekiguchi, J.M., Rathbun, G.A., Swat, W., Wang, J., et al. (1998). A critical role for DNA end-joining proteins in both lymphogenesis and neurogenesis. Cell *95*, 891–902.

Gottlieb, T.M., and Jackson, S.P. (1993). The DNA-dependent protein kinase: requirement for DNA ends and association with Ku antigen. Cell *72*, 131–142.

Grawunder, U., Wilm, M., Wu, X., Kulesza, P., Wilson, T.E., Mann, M., and Lieber, M.R. (1997). Activity of DNA ligase IV stimulated by complex formation with XRCC4 protein in mammalian cells. Nature *388*, 492–495.

Kegel, A., Sjostrand, J.O., and Astrom, S.U. (2001). Nej1p, a cell type-specific regulator of nonhomologous end joining in yeast. Curr. Biol. *11*, 1611–1617.

Ma, Y., Pannicke, U., Schwarz, K., and Lieber, M.R. (2002). Hairpin opening and overhang processing by an Artemis/DNA-dependent protein kinase complex in nonhomologous end joining and V(D)J recombination. Cell *108*, 781–794.

Matsuura, S., Tauchi, H., Nakamura, A., Kondo, N., Sakamoto, S., Endo, S., Smeets, D., Solder, B., Belohradsky, B.H., Der Kaloustian, V.M., et al. (1998). Positional cloning of the gene for Nijmegen breakage syndrome. Nat. Genet. *19*, 179–181.

Moshous, D., Callebaut, I., de Chasseval, R., Corneo, B., Cavazzana-Calvo, M., Le Deist, F., Tezcan, I., Sanal, O., Bertrand, Y., Philippe, N., et al. (2001). Artemis, a novel DNA double-strand break repair/V(D)J recombination protein, is mutated in human severe combined immune deficiency. Cell *105*, 177–186.

Moshous, D., Pannetier, C., Chasseval Rd, R., Deist Fl, F., Cavazzana-Calvo, M., Romana, S., Macintyre, E., Canioni, D., Brousse, N., Fischer, A., et al. (2003). Partial T and B lymphocyte immunodeficiency and predisposition to lymphoma in patients with hypomorphic mutations in Artemis. J. Clin. Invest. *111*, 381–387.

Nicolas, N., Moshous, D., Cavazzana-Calvo, M., Papadopoulo, D., de Chasseval, R., Le Deist, F., Fischer, A., and de Villartay, J.P. (1998). A human severe combined immunodeficiency (SCID) condition with increased sensitivity to ionizing radiations and impaired V(D)J rearrangements defines a new DNA recombination/repair deficiency. J. Exp. Med. *188*, 627–634.

O'Driscoll, M., Cerosaletti, K.M., Girard, P.M., Dai, Y., Stumm, M., Kysela, B., Hirsch, B., Gennery, A., Palmer, S.E., Seidel, J., et al. (2001). DNA ligase IV mutations identified in patients exhibiting developmental delay and immunodeficiency. Mol. Cell *8*, 1175–1185.

Ooi, S.L., Shoemaker, D.D., and Boeke, J.D. (2001). A DNA microarray-based genetic screen for nonhomologous end-joining mutants in Saccharomyces cerevisiae. Science *294*, 2552–2556.

Poinsignon, C., Moshous, D., Callebaut, I., de Chasseval, R., Villey, I., and de Villartay, J.P. (2004). The metallo-beta-lactamase/beta-CASP domain of Artemis constitutes the catalytic core for V(D)J recombination. J. Exp. Med. *199*, 315–321.

Revy, P., Buck, D., Le Deist, F., and De Villartay, J.P. (2005). The repair of DNA damages/modifications during the maturation of the immune system: lessons from human primary immunodeficiency disorders and animal models. Adv. Immunol. *87*, 237–295.

Riballo, E., Critchlow, S.E., Teo, S.H., Doherty, A.J., Priestley, A., Broughton, B., Kysela, B., Beamish, H., Plowman, N., Arlett, C.F., et al. (1999). Identification of a defect in DNA ligase IV in a radiosensitive leukaemia patient. Curr. Biol. *9*, 699–702.

Riballo, E., Doherty, A.J., Dai, Y., Stiff, T., Oettinger, M.A., Jeggo, P.A., and Kysela, B. (2001). Cellular and biochemical impact of a mutation in DNA ligase IV conferring clinical radiosensitivity. J. Biol. Chem. *276*, 31124–31132.

Robbins, P.B., Skelton, D.C., Yu, X.J., Halene, S., Leonard, E.H., and Kohn, D.B. (1998). Consistent, persistent expression from modified retroviral vectors in murine hematopoietic stem cells. Proc. Natl. Acad. Sci. USA *95*, 10182–10187.

Rogakou, E.P., Pilch, D.R., Orr, A.H., Ivanova, V.S., and Bonner, W.M. (1998). DNA double-stranded breaks induce histone H2AX phosphorylation on serine 139. J. Biol. Chem. *273*, 5858–5868.

Rooney, S., Sekiguchi, J., Zhu, C., Cheng, H.L., Manis, J., Whitlow, S., DeVido, J., Foy, D., Chaudhuri, J., Lombard, D., and Alt, F.W. (2002). Leaky Scid phenotype associated with defective V(D)J coding end processing in Artemis-deficient mice. Mol. Cell *10*, 1379–1390.

Rooney, S., Alt, F.W., Lombard, D., Whitlow, S., Eckersdorff, M., Fleming, J., Fugmann, S., Ferguson, D.O., Schatz, D.G., and Sekiguchi, J. (2003). Defective DNA repair and increased genomic instability in Artemis-deficient murine cells. J. Exp. Med. *197*, 553–565.

Sancar, A., Lindsey-Boltz, L.A., Unsal-Kacmaz, K., and Linn, S. (2004). Molecular mechanisms of mammalian DNA repair and the DNA damage checkpoints. Annu. Rev. Biochem. *73*, 39–85.

Shearer, W.T., Rosenblatt, H.M., Gelman, R.S., Oyomopito, R., Plaeger, S., Stiehm, E.R., Wara, D.W., Douglas, S.D., Luzuriaga, K., McFarland, E.J., et al. (2003). Lymphocyte subsets in healthy children from birth through 18 years of age: the Pediatric AIDS Clinical Trials Group P1009 study. J. Allergy Clin. Immunol. *112*, 973–980.

Smith, J., Riballo, E., Kysela, B., Baldeyron, C., Manolis, K., Masson, C., Lieber, M.R., Papadopoulo, D., and Jeggo, P. (2003). Impact of DNA ligase IV on the fidelity of end joining in human cells. Nucleic Acids Res. *31*, 2157–2167.

Valencia, M., Bentele, M., Vaze, M.B., Herrmann, G., Kraus, E., Lee, S.E., Schar, P., and Haber, J.E. (2001). NEJ1 controls non-homologous end joining in Saccharomyces cerevisiae. Nature *414*, 666–669.

Varon, R., Vissinga, C., Platzer, M., Cerosaletti, K.M., Chrzanowska, K.H., Saar, K., Beckmann, G., Seemanova, E., Cooper, P.R., Nowak, N.J., et al. (1998). Nibrin, a novel DNA double-strand break repair protein, is mutated in Nijmegen breakage syndrome. Cell *93*, 467–476.

Wei, Y., Yu, L., Bowen, J., Gorovsky, M.A., and Allis, C.D. (1999). Phosphorylation of histone H3 is required for proper chromosome condensation and segregation. Cell *97*, 99–109.

Accession Numbers

Human Cernunnos cDNA sequence was deposited into EMBL under accession number AJ972687.